

Terry L. Dickson,¹ Paul T. Williams,¹ B. Richard Bass,¹ Mark T. Kirk²

Preliminary Results of the United States Nuclear Regulatory Commission's Pressurized Thermal Shock Rule Reevaluation Project

Reference: Demars, K.A., Henderson, W.P., and Liu, M., “**Preliminary Results of the United States Nuclear Regulatory Commission's Pressurized Thermal Shock Rule Reevaluation Project,**” *Probabilistic Aspects of Life Prediction, ASTM STP # 1450*, W. S. Johnson and B. M. Hillberry, Eds., ASTM International, West Conshohocken, PA, 2003.

Abstract: The current federal regulations to insure that nuclear reactor pressure vessels (RPVs) maintain their structural integrity when subjected to transients such as pressurized thermal shock (PTS) events were derived from computational models developed in the early to mid-1980s. Since that time, there have been advancements in relevant technologies associated with the physics of PTS events that impact RPV integrity assessment. Preliminary studies performed in 1999 suggested that application of an improved technology could reduce the conservatism in the current regulations while continuing to provide reasonable assurance of adequate protection to public health and safety. A relaxation of PTS regulations could have profound implications for plant license-extension considerations. Based on the above, the United States Nuclear Regulatory Commission (USNRC) initiated in 1999 a program to re-evaluate the current PTS regulations within the framework established by modern probabilistic risk assessment techniques.

As part of the USNRC PTS project, improved computational models have evolved through interactions between experts in the relevant disciplines of thermal hydraulics, probabilistic risk assessment, human reliability analysis, materials embrittlement effects on fracture toughness (crack initiation and arrest), fracture mechanics methodology, and fabrication-induced flaw characterization. The experts have been from the NRC staff, their contractors, and representatives from the nuclear industry. These improved models have been implemented into the FAVOR (Fracture Analysis of Vessels: Oak Ridge) computer code which is an applications tool for performing risk-informed structural integrity evaluations of embrittled RPVs subjected to transient thermal-hydraulic loading conditions.

Recently, the FAVOR code was applied to a domestic commercial pressurized water reactor to evaluate the adequacy of the current regulations and to determine if a technical basis can be established to support a change in the current regulations. This paper gives an overview of the improved computational methodology and presents some results of the preliminary analyses.

Keywords: fracture mechanics, pressurized thermal shock, probabilistic, Monte Carlo

¹ Computational Sciences and Engineering Division, Oak Ridge National Laboratory, P.O. Box 2009, Mail Stop 8056, Oak Ridge, TN 37831-8056.

² Office of Nuclear Regulatory Research, United States Nuclear Regulatory Commission, Mail Stop T10-E1, Washington, DC 20555-0001.

Problem Definition, Current PTS Regulations, and Overview of PTS Reevaluation Project

The issue of pressurized thermal shock (PTS) in nuclear reactor pressure vessels (RPVs) arises because cumulative neutron irradiation exposure makes the RPV more brittle (i.e., reduced ductility and fracture toughness) and, therefore, increasingly susceptible to cleavage (brittle) fracture over its operating life. The degree of embrittlement of RPV steel is quantified by changes in the reference nil-ductility transition temperature, RT_{NDT} . The radiation-induced shift in RT_{NDT} is a function of the chemical composition of the steel, the neutron irradiation exposure, and the initial unirradiated transition temperature, RT_{NDT0} .

In pressurized water reactors (PWRs), transients can occur that result in a severe overcooling (thermal shock) of the RPV concurrent with or followed by high repressurization. If an aging RPV is subjected to a PTS event, flaws on or near the inner surface could initiate in cleavage fracture and propagate through the RPV wall, thus introducing the possibility of RPV failure. Figures 1(a) and (b) illustrate a specific postulated PTS event: Figure 1(a) gives the thermal-hydraulic boundary condition to be imposed on the inner surface of an RPV and Figure 1(b) shows the probability density distribution of the transient frequency (in events per operating reactor year). This specific transient is designated as *Postulated Transient 113* and will be discussed in more detail in the following.

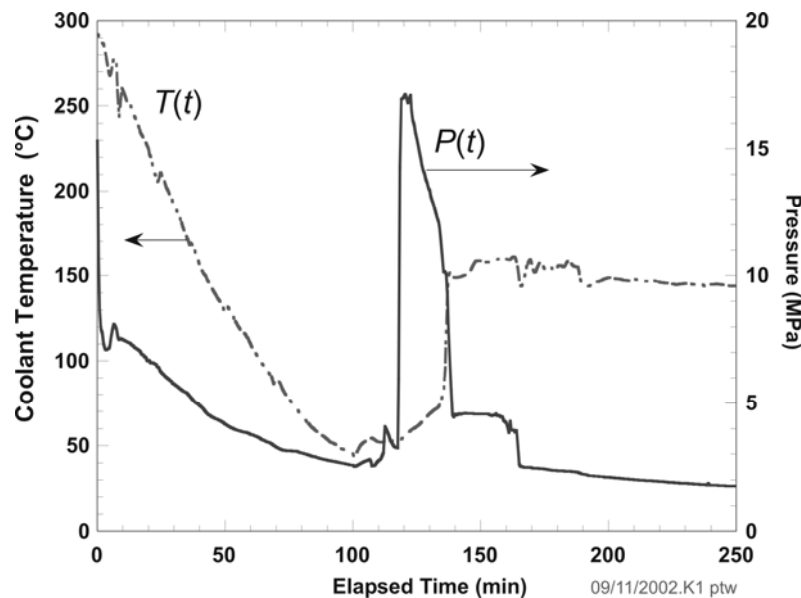


Figure 1 (a) *Postulated Transient 113 (a) Thermal-Hydraulic Boundary Conditions Imposed on RPV Inner Surface*

The relevant current regulations are the *PTS Rule* [1] and United States Nuclear Regulatory Commission (USNRC) Regulatory Guide (RG) 1.154 [2]. The PTS rule establishes screening criteria in the form of limiting values of RT_{NDT} . The current PTS screening criteria are values of RT_{NDT} at the inner surface of the RPV of 270 °F (132.2 °C) for plates, forgings, and axial welds, and 300 °F (148.9 °C) for circumferential welds.

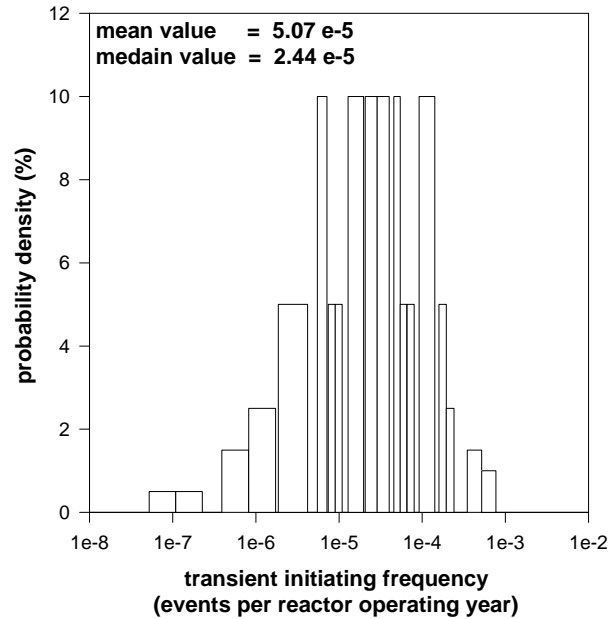


Figure 1 (b) Probability Density Distribution for Transient Initiating Frequency of Transient 113

The PTS rule requires plants that desire to operate beyond the screening criteria to submit an integrated plant-specific safety analysis to the NRC three years before the PTS screening limit is anticipated to be reached for any material in the RPV beltline. Regulatory Guide 1.154 provides guidance regarding an acceptable analysis methodology. Probabilistic fracture mechanics (PFM) analysis is a major part of that methodology. The objective of performing an RG 1.154 analysis is to demonstrate that the frequency of RPV failure per reactor year of operation due to PTS is less than the current acceptance criterion of 5×10^{-6} failures per reactor-operating year. The value of 5×10^{-6} RPV failures per reactor year is also currently being re-examined by NRC staff and could be modified.

Preliminary studies performed in 1999 [3] suggested that application of an improved technology, developed since the current regulations were derived in the early to mid-1980s, could reduce the conservatism in the current regulations while continuing to provide reasonable assurance of adequate protection to public health and safety. A relaxation of PTS regulations could have profound implications for plant license-extension considerations. Based on the above, the USNRC is currently re-evaluating the current PTS regulations within the framework established by modern probabilistic risk assessment (PRA) techniques.

An objective of the PTS re-evaluation program is to cover the range of various system designs, operational procedures, and training programs. The plan is to perform analyses for four domestic commercial PWRs. Other analyses will be performed as necessary so that any revision to the PTS rule may be applied generically to all domestic commercial PWRs. The updated technology in the FAVOR code was recently applied for the first time to a commercial PWR. For purposes of discussion, in this paper, the subject plant will be referred to as *Plant X*.

Overview of PTS Analysis

The evaluation of a PTS event involves complex interactions among many variables impacting the behavior of flaws postulated to exist on (or near) the inner surface of an aging RPV subjected to a PTS event. Varying degrees of uncertainty are associated with the variables that are input into a PTS analysis; therefore, a probabilistic risk assessment (PRA) methodology is applied to evaluate the risk of RPV fracture (crack initiation) and potential failure, where the results of these analyses, when compared with the limit of acceptable failure probability, provide an estimate of the residual life of an RPV. Also, results of such analyses can be used to evaluate the potential benefits of plant-specific mitigating actions designed to reduce the probability of RPV failure, thus potentially extending the operating life of the RPV.

Definition of RPV Beltline Region and Embrittlement Map

The PTS analysis is performed for the beltline of an RPV, usually assumed to extend from one foot below the reactor core to one foot above the reactor core as illustrated in Figure 2.

For the PTS analysis of *Plant X*, detailed neutron fluence maps were provided by Brookhaven National Laboratory (BNL) corresponding to 32 and 40 effective-full-power years (EFPY). Neutron fluence maps for times in the operating life of the RPV later than 40 EFPY were obtained by linear extrapolation from the maps for 32 and 40 EFPY. The assumption associated with this extrapolation is that the current core refueling scheme (at 18 EFPY) is maintained. This assumption is also implicit in the fluence maps for 32 and 40 EFPY.

Each of the fluence maps contained 13 080 discrete values of neutron fluence (60 azimuthal \times 218 axial) corresponding to one-eighth of the RPV azimuth (45-degree sector); therefore, the entire 360-degree beltline region would have to be discretized into 104 640 subregions to accommodate the level of detail provided by BNL. In practice, one may take advantage of symmetry to include this amount of detail with a considerably smaller number of subregions.

The modeling and procedures used in generating these neutron fluence maps were based on the guidance provided in the NRC Regulatory Guide 1.190 [4]. The calculations were performed using the DORT discrete ordinates transport code [5] and the BUGLE-93 [6] forty-seven neutron group ENDF/B-VI nuclear cross sections and fission spectra.

The FAVOR code allows for the RPV beltline to be divided into major regions such as axial welds, circumferential welds, and plates or forgings such that each may have its own embrittlement-sensitive chemistry. The major regions may be further divided into subregions to accommodate detailed neutron fluence maps. Figure 3 illustrates the layout of the RPV beltline for *Plant X* to be discussed in this paper.

Table 1 provides a breakdown of the RPV beltline into major regions, with the respective chemistries, unirradiated values of RT_{NDT} (RT_{NDT_0}), number of subregions into which the major regions are further discretized (to accommodate the detailed neutron fluence maps provided by BNL), etc. The most-limiting embrittled region in the RPV beltline is the circumferential weld 1229 which, as illustrated in Table 1, has an RT_{PTS} at the inner surface of the RPV at 60 EFPY, of 115.6 °C. The value of RT_{PTS} is RT_{NDT} plus a margin term of 32.3 °C, to account for uncertainties in the initial unirradiated value of RT_{NDT_0} and the correlation used to predict the radiation-induced shift in RT_{NDT} .

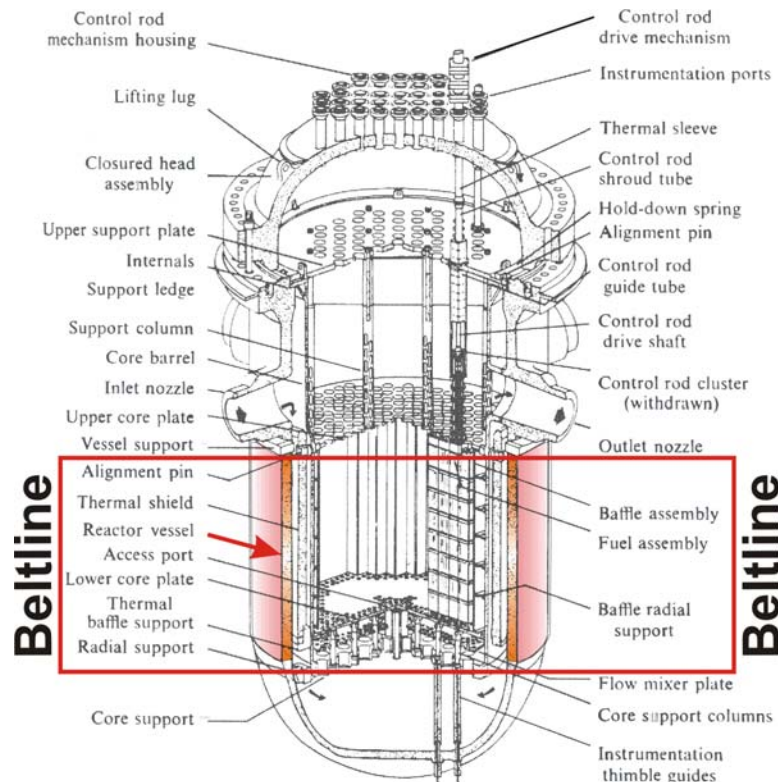


Figure 2 – The Beltline Region of an RPV Wall

Generation of Transient Data

A comprehensive search for transients that are both probabilistically credible and physically significant is necessary. PRA is used to guide the choice of selected transients for thermal hydraulic analysis. There is feedback to PRA from thermal hydraulics and fracture mechanics analyses to determine not only the probability of occurrence of a given sequence but also its risk significance. Scenario screening integrates the knowledge from the three disciplines of PRA, thermal hydraulics, and fracture mechanics.

For the PTS analysis of *Plant X*, Information Sciences Laboratories (ISL) provided thermal hydraulic boundary conditions for 55 transient conditions. The selection of these 55 conditions was based on not only thermal hydraulic and anticipated fracture mechanics considerations, but also on PRA input regarding scenarios of sufficient likelihood to be of potential concern to PTS. The thermal-hydraulic calculations were performed using the RELAP5/MOD3 code [7]. The specific transients were selected by considering the thermal hydraulic system behavior, as well as possible plant equipment failures, plant operating procedures, and human reliability issues [8]. For each of the 55 transients, ISL provided a convective heat-transfer-coefficient time history, a coolant-temperature time history, and a pressure time history. Each of the time histories consisted of 500 time history pairs. The time-history pairs were equally spaced by 30 seconds; therefore, the total duration of each of the transients was 250 minutes. Figure 1(a) illustrates the thermal hydraulic boundary condition to be imposed on the inner surface of the RPV for *Postulated Transient 113*, which is the dominant postulated transient for *Plant X*, as will be discussed below.

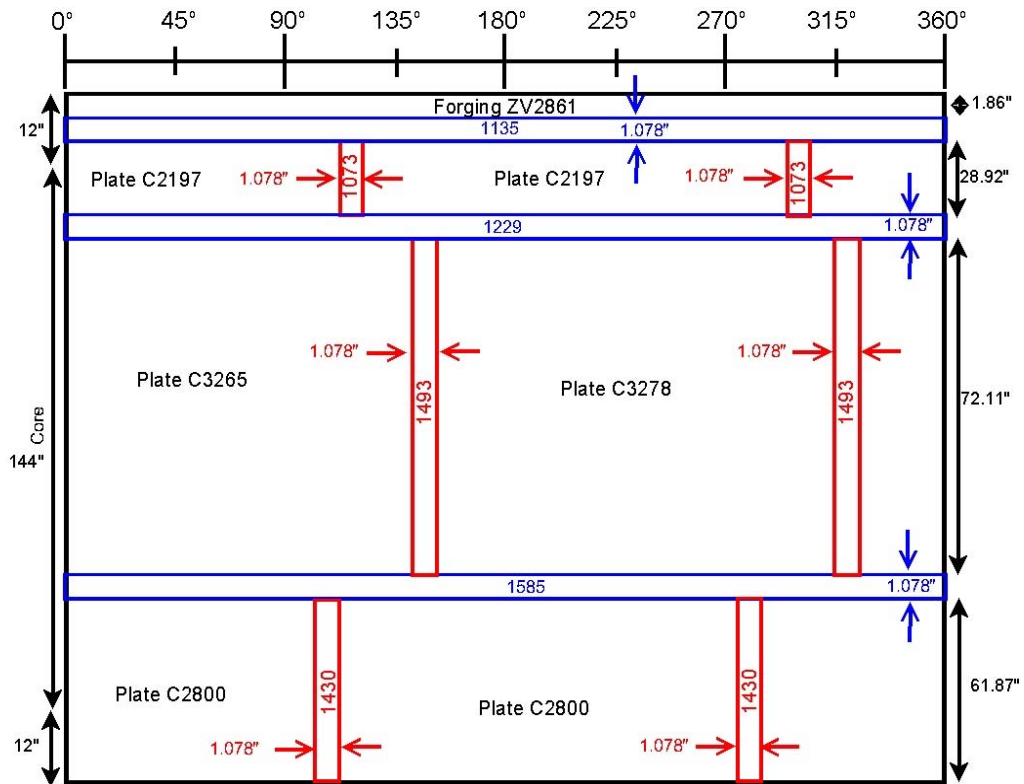


Figure 3 – Layout of the RPV Beltline for Plant X

Table 1 – RPV Beltline Model Data Used in PTS Analysis of Plant X

			Number	Percent	Chemistry Content			At 60 EFPY	
Major	RPV	Region	of RPV	of Total				RT_{NDT0}	$RT_{PTS(max)}$
Number	Description	Heat	Subregions	Flaws	wt% Cu	wt% Ni	wt% P	(°C)	(°C)
1	axial weld	1430	77	2.68	0.19	0.57	0.017	-20.6	97.0
2	axial weld	1493	85	3.12	0.19	0.57	0.017	-20.6	96.2
3	axial weld	1073	49	1.26	0.21	0.64	0.025	-20.6	111.6
4	circ. weld	1585	480	11.6	0.22	0.54	0.016	-20.6	105.3
5	circ. weld	1229	480	11.6	0.23	0.59	0.021	-12.2	115.6
6	circ. weld	1135	480	11.6	0.23	0.52	0.011	-20.6	80.0
7	plate	C2800	4620	21.7	0.11	0.63	0.012	-17.2	64.4
8	plate	C3265	5100	12.6	0.1	0.5	0.015	-17.2	60.1
9	plate	C3278	5100	12.6	0.12	0.6	0.01	-17.2	65.5
10	plate	C2197	2940	10.2	0.15	0.5	0.008	-17.2	68.6
11	forging	ZV2861	240	0.65	0.16	0.65	0.006	-16.1	58.4

For the PTS analysis of *Plant X*, Sandia National Laboratory (SNL) provided a probability distribution of the transient frequency (events per reactor-operating year) for each of the 55 transients. The SAPHIRE Version 7 [9] code was used to generate the probability distributions using 20 bins per transient.

The relevant transients were developed from a PRA model for *Plant X* that addressed possible over-cooling transients. The identification of these over-cooling scenarios considered the earlier 1980s work, as well as a review of the current plant design, recent operating history, latest procedures, present-day operator training, and feedback from the

ongoing thermal-hydraulic analyses. The PRA model development involved two visits to the plant, where plant staff input was obtained and plant staff comments on the PRA, including the human reliability assessments, were received and incorporated. Additionally, during the first visit, over-cooling events were simulated on the plant simulator to gain insights about operator responses to such events.

Flaw-Characterization Data

Perhaps the single largest improvement in the updated computational methodology is the establishment of a technical basis for the postulation of flaws. The PFM model utilized in the analyses from which the current PTS regulations were derived [10] conservatively postulated that all fabrication flaws were inner-surface-breaking flaws.

The USNRC has supported research at Pacific Northwest National Laboratory (PNNL) that has resulted in the postulation of fabrication flaws based on the non-destructive and destructive examination of actual RPV material. Such measurements have been used to characterize the number, size, and location of flaws in various types of weld and base metal used to fabricate vessels, thus providing a technical basis for the flaw data, which is critical input data into FAVOR analyses. These measurements have been supplemented by expert elicitation [11]. Separate probability distributions have been developed to characterize the number, size, and location (in the RPV wall) of flaws in different regions of the RPV. The regions include the main seam welds, repair welds, base metal of plates and forgings, and the cladding as applied to the inner surface of the vessel. The reader is referred to [12-15] for the details of this research.

Figure 4 illustrates an inner-surface-breaking and an embedded flaw. An inner-surface-breaking flaw of a specific size has a greater fracture-mechanics significance, i.e., is much more likely to result in cleavage fracture than an embedded flaw of the same size. A major result of the PNNL flaw-characterization research is that RPV material has a much higher density of flaws per volume of RPV material than was postulated in the analyses from which the current PTS regulations were derived; however, all of the flaws detected thus far have been embedded.

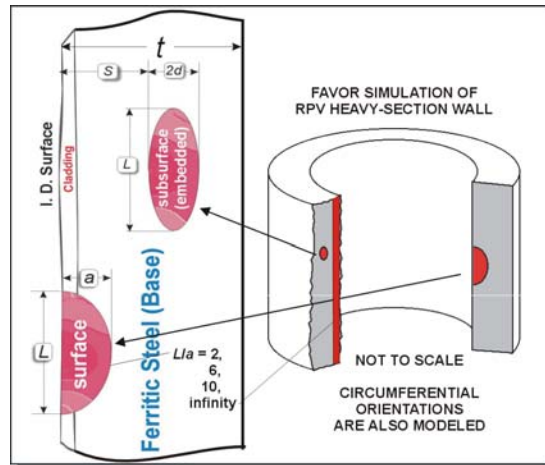


Figure 4 – Flaw Models In PTS Analysis Include Inner Surface-Breaking Flaws and Fully Elliptic Embedded Flaws

Computational Methodology

Figure 5 is a flow chart that illustrates the essential elements of the FAVOR PFM methodology which is based on the Monte Carlo technique, i.e., deterministic fracture analyses are performed on a large number of stochastically-generated RPV trials. The outer-most loop is indexed for each RPV trial included in the analysis.

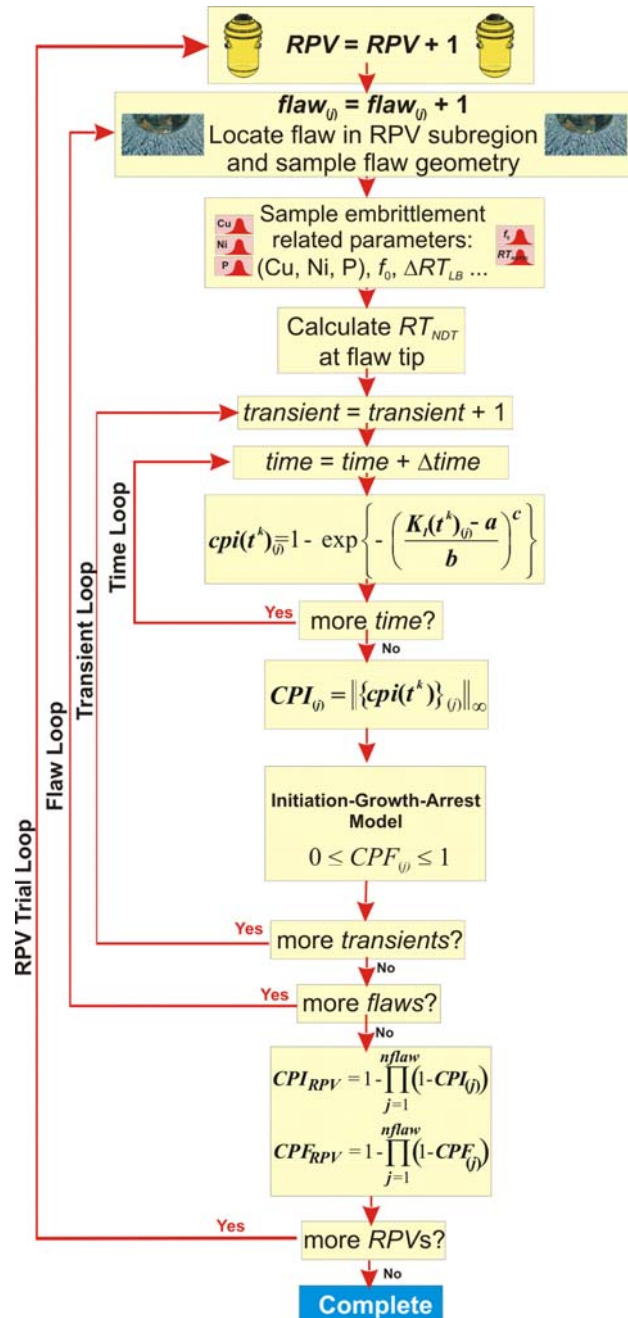


Figure 5 – Flowchart Showing the Essential Elements of PFM Analysis

Since each RPV trial can be postulated to contain multiple flaws, the next inner-most loop is indexed for the number of flaws. Each postulated flaw is located in a particular

RPV beltline subregion that has its own distinguishing embrittlement-related parameters. Next, the flaw geometry (depth, length, and location in the RPV wall) is determined by sampling from appropriate distributions derived from expert judgment and non-destructive and destructive examination of RPV material. Each of the embrittlement-related parameters (weight-percent of copper, weight-percent of nickel, weight-percent of phosphorus, neutron fluence, and RT_{NDT0}) are sampled from appropriate distributions about best-estimate values. The neutron fluence is attenuated to the crack tip location and the value of RT_{NDT} is calculated. Then a deterministic fracture analysis is performed on the current flaw for each of the postulated PTS transients. The temporal relationship between the applied Mode I stress intensity factor (K_I) and the static cleavage fracture initiation toughness (K_{Ic}) at the crack tip is calculated at discrete transient time steps. The fracture initiation toughness, K_{Ic} , is a function of the normalized temperature, $T(t)-RT_{NDT}$, where $T(t)$ is the time-dependent temperature at the crack tip. Analysis results are used to calculate the conditional probability of initiation (CPI) for each postulated flaw, i.e., the probability that pre-existing fabrication flaw(s) will initiate in cleavage fracture. Also, the PFM model calculates the conditional probability of failure (CPF), i.e., probability that an initiated flaw will propagate through the RPV wall. The probabilities are conditional in the sense that the postulated transients are assumed to occur and the postulated flaws are assumed to exist.

Calculation of the Conditional Probability of Crack Initiation (CPI)

As discussed above, a deterministic fracture analysis is performed by stepping through discrete transient time steps to examine the temporal relationship between the applied Mode I stress intensity factor (K_I) and the static cleavage fracture initiation toughness (K_{Ic}) at the crack tip. A Weibull distribution, in which the parameters were calculated by the *Method of Moments* point-estimation technique, forms the basis for the statistical models for fracture initiation (K_{Ic}) and crack arrest (K_{Ia}) toughness [16].

Figure 6 illustrates the Weibull distribution for K_{Ic} , for which there are three parameters to estimate; the location parameter a , of the random variate, the scale, b , of the random variate, and the shape parameter, c . The Weibull probability density, w , is given by:

$$w(x|a,b,c) = \frac{c}{b} y^{c-1} \exp(-y^c), \quad (y = (x-a)/b, x > a, b, c > 0) \quad (1)$$

where the parameters a , b , and c of the distribution are a function of $(T(t) - RT_{NDT})$.

A deterministic fracture analysis is performed for each flaw by stepping through the transient time history for each transient. At each time step, an instantaneous $cpi(t)_{(j)}$ is calculated for the j th flaw from the Weibull K_{Ic} cumulative distribution function at time, t , for the fractional part (percentile) of the distribution that corresponds to the applied $K_I(t)_{(j)}$:

$$\Pr(K_{Ic} \leq K_I(t)_{(j)}) = cpi(t)_{(j)} = 1 - \exp\left\{-\left(\frac{K_I(t)_{(j)} - a}{b}\right)^c\right\} \quad (2)$$

Here, $cpi(t)_{(j)}$ is the instantaneous conditional probability of initiation at the crack tip at time t . Figure 6 illustrates an example of the interaction of the applied K_I time history and the Weibull K_{Ic} statistical distribution. In this illustration, at a transient time of 26 minutes, the applied K_I of $62.96 \text{ MPa}\cdot\text{m}^{1/2}$ corresponds to the 34.93 percentile K_{Ic} curve, i.e., the applied K_I corresponds to 0.3493 of the area under the Weibull K_{Ic} distribution for $T(t) - RT_{NDT} = -28.8 \text{ }^\circ\text{C}$; therefore, the instantaneous conditional probability of crack initiation at this time step is 0.3493.

For the j th flaw, $CPI_{(j)}$ is the maximum of the vector $\{cpi(t^k)\}_{(j)}$ over all transient time steps. For the example flaw in Figure 6, $CPI_{(j)} = 0.3943$ occurs at a transient time of 26 minutes.

In Figure 6, the line designated as “a” is the Weibull location parameter which is the lowest possible value of K_{Ic} . If for any flaw the applied K_I never exceeds the Weibull location parameter through all transient time, then $CPI_{(j)} = 0$. The value of $CPI_{(j)}$ may be thought of as “to what percentile” into the K_{Ic} space does the applied K_I penetrate.

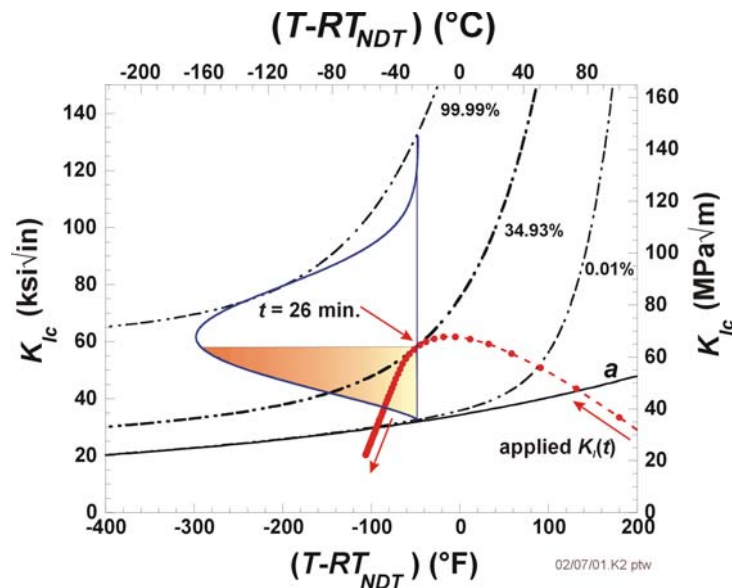


Figure 6 – Interaction of the Applied K_I Time History and the Weibull K_{Ic} Statistical Model for the Example Flaw.

Calculation of RPV Failure in the PFM Model

A flaw initiated in cleavage fracture has two possible outcomes during the duration of the transient. It either propagates through the entire wall thickness causing RPV failure, or it experiences a stable arrest at a location in the wall. In either case, the advancement of the crack tip through the RPV wall may involve a sequence of initiation / arrest / reinitiation events. The details regarding the calculation of the conditional probability of RPV failure (CPF) for each flaw are fairly complex and can not be addressed in this paper due to space limitations. The reader is referred to [17] for details regarding the computational model to calculate CPF for each flaw

Warm Prestressing

A phenomenon known as warm-prestress (WPS) is available in FAVOR as a user-option. The concept of the WPS effect is that a crack tip cannot initiate in cleavage fracture in a stress field that is decreasing with respect to time.

If WPS is applied, then two conditions must be satisfied in order that a flaw have a finite conditional probability of initiation (CPI) at any transient time step:

- (1) K_I must be greater than the Weibull location parameter “ a ” for the K_{Ic} distribution, and
- (2) K_I must be greater than the previous maximum K_I for all previous time steps in the transient.

If the WPS option is not applied, only the first condition must be satisfied to have a CPI greater than zero.

In the illustrative example and in Figure 6, the maximum applied K_I of 67.91 MPa-m^{1/2} occurred at a transient time of 16 minutes. If the WPS option had been activated, the maximum applied K_I of 67.91 MPa m^{1/2} would correspond to the 16.79 percentile K_{Ic} curve, i.e., the applied K_I corresponds to 0.1679 of the area under the Weibull K_{Ic} probability density distribution for $T(t) - RT_{NDT} = -2.9$ °C. Therefore, if WPS is applied, $CPI_{(j)}$ is the maximum of the vector $\{cpi(t^k)\}_{(j)}$ over all transient time steps up to the time of the maximum applied K_I .

The WPS effect can also impact the through-wall analyses to determine if a flaw, initiated in cleavage fracture, propagates through the wall to RPV failure. If the WPS option is activated, for an arrested flaw to reinitiate at a later transient time, two conditions must be satisfied:

- (1) K_I must be greater than K_{Ic} (from a sampled Weibull percentile K_{Ic} curve), and
- (2) K_I must be greater than the previous maximum applied K_I (for the arrested flaw depth) at discrete transient time steps equal to or greater than the discrete time step currently being analyzed.

If WPS is not specified, only the first condition must be satisfied to reinitiate an arrested flaw.

Treatment of Multiple Flaws in the PFM Model

For each RPV, the process described above is repeated for each postulated flaw, resulting in an array of values of $CPI_{(j)}$, one for each flaw, where each value of $CPI_{(j)}$ is the maximum of the vector $\{cpi(t^k)\}_{(j)}$ over all transient time steps if WPS is not applied, or, if WPS is applied, over the maximum of the vector $\{cpi(t^k)\}_{(j)}$ for the transient time steps up to the time corresponding to the maximum applied K_I .

If $CPI_{(1)}$ is the probability of fracture of a flaw in an RPV that contains a single flaw, then $(1-CPI_{(1)})$ is the probability of non-initiation for that RPV. If $CPI_{(1)}$ and $CPI_{(2)}$ are the probabilities of fracture of two flaws in an RPV that contains two flaws, then $(1-CPI_{(1)}) (1-CPI_{(2)})$ is the probability of non-initiation of that RPV, i.e., the probability that neither of the two flaws will fracture. This can be generalized to an RPV with n_{flaw} flaws, so that the joint probability that none of the flaws will fracture is:

$$\left. \begin{array}{l} \text{Conditional probability} \\ \text{of non-initiation} \end{array} \right\} = \prod_{j=1}^{nflaw} (1 - CPI_{(j)}) \quad (3)$$

$$= (1 - CPI_{(1)})(1 - CPI_{(2)}) \dots (1 - CPI_{(nflaw)})$$

Therefore, for an RPV with $nflaw$ flaws, the probability that at least one of the $nflaw$ flaws will fracture is:

$$CPI_{RPV} = 1 - \prod_{j=1}^{nflaw} (1 - CPI_j) \quad (4)$$

$$= 1 - [(1 - CPI_1)(1 - CPI_2) \dots (1 - CPI_{nflaw})]$$

The method described here for combining the values of CPI for multiple flaws in an RPV is also used for combining the values of CPF for multiple flaws.

Integration of Results of PFM Analysis with Probability Distributions for Transient Initiating Frequency

Final results of the PFM analysis are (1) an (j,i) array, designated as the $PFMI$ array, of values of CPI , where each entry in the array is the value of conditional probability of crack initiation for the i th simulated RPV subjected the j^{th} postulated transient (2) an (j,i) array, designated as the $PFMF$ array, of values of CPF where each entry in the array is the value of conditional probability of RPV failure of the i^{th} simulated RPV subjected the j^{th} postulated transient.

The probability distributions of the transient initiating frequencies (example illustrated in Figure 1(b)) of all transients included in the PTS analysis are integrated with the results of the PFM analysis (contained in the $PFMI$ and $PFMF$ as defined above) to produce probability distributions for the frequency of crack initiation and the frequency of RPV failure.

For each simulated RPV, values of transient initiating frequency are sampled from their respective distribution for each transient, resulting in a row vector $\phi(E)$ of initiating frequencies. The inner product of the row vector of the sampled initiating frequencies (events per reactor-operating year) and the i^{th} column vector of $PFMI$ (crack initiations per transient event) produces the frequency of crack initiation of the i^{th} simulated RPV (crack initiations per reactor-operating year), designated as $\Phi(I)_{(i)}$.

$$\Phi(I)_{(i)} = \sum_{j=1}^{N_{TRAN}} \phi(E)_{(j)} PFMI(j,i) \quad (5)$$

$$\Phi(F)_{(i)} = \sum_{j=1}^{N_{TRAN}} \phi(E)_{(j)} PFMF(j,i)$$

Likewise, the inner product of the row vector of sampled transient initiating frequencies and the i th column vector of $PFMF$ results in the frequency of failure of the i th simulated RPV (failures per reactor operating year), designated as $\Phi(F)_{(i)}$.

At the end of the process, there are discrete distributions for the frequency of crack initiation and frequency of RPV failure.

PTS Analysis Results of Plant X

Table 2 is a summary of the risk-informed PTS analysis results of *Plant X*, which contains mean values of the probability distributions of the frequency of crack initiation (*FCI*) and the frequency of RPV failure (*FVF*) at increasing time in the operating life of the RPV (as quantified by EFPY and limiting RT_{PTS}). Values are provided for the cases of with and without the WPS effect applied in the PFM analysis.

Analyses were performed, without WPS, at nine levels of embrittlement, each one in principal, corresponding to a particular point in the operating life of the RPV. The first two analysis results correspond to the neutron fluence maps of 32 and 40 EFPY, which were provided by BNL as previously discussed.

The neutron fluence maps for the additional levels of embrittlement (seven times in the RPV operating life) were obtained by linearly extrapolating beyond these two maps. Clearly, some of these extrapolations are far beyond the range of EFPY for which *Plant X* would ever actually operate. They were performed since an objective of the analysis was to determine the level of embrittlement that corresponds to a frequency of RPV failure in the 10^{-6} - 10^{-7} failures per reactor-operating year range.

Figure 7 presents mean *FCI* and *FVF* results as a function of limiting RT_{PTS} . Table 3 is a summary of the PFM analysis results of the 13 dominant transients, i.e., those transients that contribute most significantly to the frequency of RPV failure. *Postulated Transient 113* is the most dominant of all the transients since it contributes 34.6 percent of the total frequency of RPV failure. A distinguishing feature of this most dominant transient is that it has a late repressurization. The coolant and pressure time histories of *Postulated Transient 113* are illustrated in Figure 1(a). The probability distribution of the initiating frequency for this transient is illustrated in Figure 1(b). The combination of the transient severity and the frequency with which it is predicted to occur determines the dominance of the transient.

Table 2 - *PTS Analysis Results for Plant X: Mean Frequency of Crack Initiation and Mean Frequency of RPV Failure as a Function of EFPY and Limiting RT_{PTS}*

		Mean Freq.	Mean Freq.		Mean Freq.	Mean Freq.	
	Limiting	of Crack	of Crack	Ratio of	of RPV	of RPV	Ratio of
EFPY	RT_{PTS}	Initiation ⁽¹⁾	Initiation	(no WPS)	Failure ⁽²⁾	Failure	(no WPS)
	(°C)	(no WPS)	(with WPS)	WPS	(no WPS)	(with WPS)	WPS
32	105.98	1.06E-08			1.48E-09		
40	109.66	1.62E-08			2.55E-09		
60	115.62	3.64E-08	9.05E-09	4.02	5.30E-09	2.09E-09	2.54
100	122.44	7.41E-08			1.17E-08		
300	138.42	3.35E-07			4.72E-08		
500	147.98	7.10E-07	3.32E-07	2.14	1.04E-07	3.64E-08	2.86
650	153.73	1.11E-06			1.46E-07		
800	158.76	1.57E-06			2.07E-07		
1000	164.71	2.43E-06	1.26E-06	1.93	3.26E-07	1.25E-07	2.61

⁽¹⁾ frequency of crack initiation (due to PTS) expressed in cracked RPVs per reactor-operating year

⁽²⁾ frequency of RPV failure (due to PTS) expressed in cracked RPVs per reactor-operating year

Table 3 – Dominant Transients for Plant X: PFM Results Evaluated at 60 EFPY (without warm Prestress)

Transient Sequence Number	Mean CPI	Mean CPF	Mean Initiating Frequency (events/year)	Percent of Total Frequency of Crack Initiation	Percent of Total Frequency of RPV Failure
113	3.46E-05	3.26E-05	5.07 e-5	5.41	34.6
122	9.74E-05	9.27E-05	7.57 e-6	2.37	15.43
164	5.70E-04	3.60E-05	1.59 e-5	28.4	11.02
109	3.26E-05	3.02E-05	9.58 e-6	1.28	8.1
160	4.38E-04	2.79E-05	1.36 e-5	22.8	7.59
165	1.47E-04	1.43E-04	1.76 e-6	0.76	5.09
141	7.23E-05	4.68E-06	5.49 e-5	11.15	4.81
156	6.53E-04	4.25E-05	5.02E-06	11.66	4.41
154	3.88E-05	2.18E-06	6.95E-05	7.46	2.95
124	1.76E-05	1.59E-05	7.57E-06	0.43	2.69
172	3.89E-05	2.20E-06	5.49E-05	5.99	2.28
121	1.75E-05	1.21E-06	3.07E-05	1.55	0.73
110	8.33E-05	4.87E-06	2.99E-06	0.74	0.29

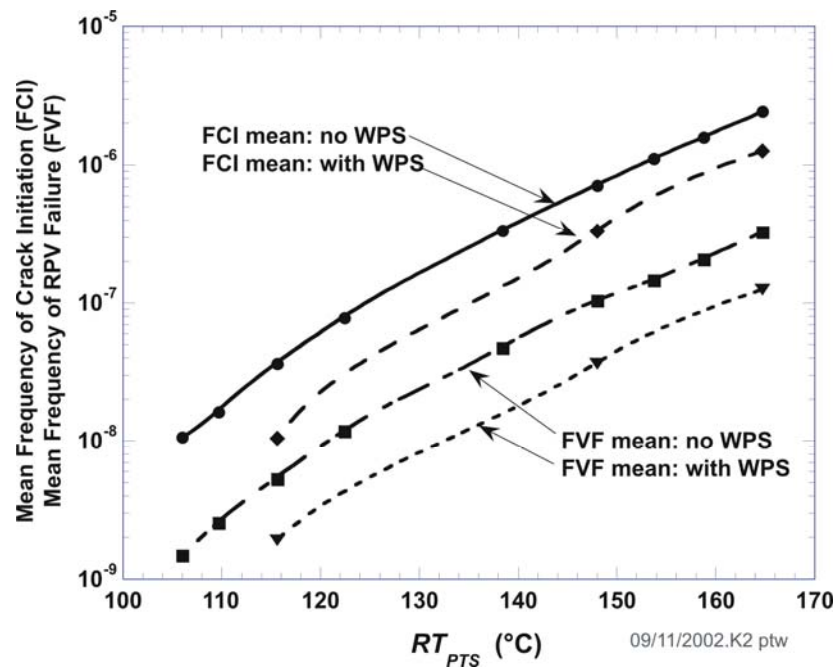


Figure 7 – PTS Results for Plant X : Mean FCI and Mean FVF vs Limiting RT_{PTS}

Summary

As part of the United States Nuclear Regulatory Commission PTS Rule Re-evaluation Project, an updated risk-informed computational methodology has evolved through interactions between experts from the NRC staff, their contractors, and representatives from the nuclear industry. An objective of the PTS Re-evaluation Project is to establish a technical basis rule within the framework established by modern probabilistic risk assessment techniques and advances in technologies associated with the physics of the PTS events. A relaxation of the current PTS regulations could have profound implications for plant license extension considerations

The updated risk-informed computational methodology has been integrated into the FAVOR code, which was recently applied to an actual PWR vessel. The mean value of the frequencies of RPV failure are 1.25×10^{-7} and 3.26×10^{-7} failures per reactor-operating year, with and without warm prestressing, respectively, when the limiting beltline value of RT_{PTS} is 328 °F (164.4 °C). The 95th percentiles of the frequencies of RPV failure are 2.10×10^{-7} and 4.23×10^{-6} failures per reactor year, with and without warm prestressing, respectively, at the same level of embrittlement.

Even though it is premature to draw any general conclusions, the preliminary results of the PTS analysis of *Plant X* provide encouragement that the application of the state-of-the-art technology will establish a technical basis for a potential relaxation of the current PTS regulations for commercial PWRs. The PTS analysis of three other PWRs is now proceeding

Disclaimer

The views expressed in this paper are those of the authors and should not be construed as the USNRC's official position.

References

- [1] Code of Federal Regulations, Title 10 (Energy), Part 50, Section 50.61 and Appendix G, 2001.
- [2] U.S. Nuclear Regulatory Commission, Regulatory Guide 1.154, Format and Content of Plant-Specific Pressurized Thermal Shock Safety Analysis Reports for Pressurized Water Reactors, 1987.
- [3] Dickson, T.L., Malik, S. N. M., Bryson, J. W., and Simonen, F. A., "Revisiting the Integrated Pressurized Thermal Shock Studies of an Aging Pressurized Water Reactor," ASME PVP-Volume 388, *Fracture, Design Analysis of Pressure Vessels, Heat Exchangers, Piping Components, and Fitness for Service, ASME Pressure Vessels and Piping Conference*, August 1999.
- [4] U.S. Nuclear Regulatory Commission, "Calculational and Dosimetry Methods for Determining Pressure Vessel Neutron Fluence," Regulatory Guide 1.190, March 2001.
- [5] *DORT, Two-Dimensional Discrete Ordinates Transport Code*, RSIC Computer Code Collection, CCC-484, Oak Ridge National Laboratory, 1988.
- [6] D. T. Ingersoll, J. E. White, R. Q. Wright, H. T. Hunter, C. O. Slater, N. M. Greene, R. E. MacFarlane, R. W. Roussin, "Production and Testing of the VITAMIN-B6

- Fine-Group and the BUGLE-93 Broad-Group Neutron/Photon Cross-section Libraries Derived from ENDF/B-VI Nuclear Data,” ORNL-6795, NUREG/CR-6214, January 1995.
- [7] Arcieri W.C., Beaton, R., Lee, T. Bessette, D.E., “RELAP5 Thermal Hydraulic Analysis to Support PTS Evaluations for the Plant X Nuclear Power Plant, Draft NUREG/CR Report, January 2001.
- [8] *Technical Basis and Implementation Guidelines for A Technique for Human Event Analysis (ATHEANA)*, USNRC – Division of Risk Analysis and Applications, Office of Nuclear Regulatory Research, NUREG-1624, Revision 1, May 2000.
- [9] Smith, C. L., et al, *Testing, Verifying and Validating SAPHIRE Versions 6.0 and 7.0*, NUREG/CR-6688, October 2000.
- [10] U.S. Nuclear Regulatory Policy Issue, 1982, NRC Staff Evaluation of Pressurized Thermal Shock, SECY 82-465.
- [11] Jackson, D.A., and Abramson, L., 1999, *Report on the Results of the Expert Judgment Process for the Generalized Flaw Size and Density Distribution for Domestic Reactor Pressure Vessels*, U.S. Nuclear Regulatory Commission Office of Research, FY 2000-2001 Operating Milestone 1A1ACE.
- [12] Schuster, G.J., Doctor, S.R., Crawford, S.L., and Pardini, A.F., 1998, *Characterization of Flaws in U.S. Reactor Pressure Vessels: Density and Distribution of Flaw Indications in PVRUF*, USNRC Report NUREG/CR-6471, Vol. 1, U.S. Nuclear Regulatory Commission, Washington, D.C.
- [13] Schuster, G.J., Doctor, S.R., and Heasler, P.G., 2000, *Characterization of Flaws in U.S. Reactor Pressure Vessels: Validation of Flaw Density and Distribution in the Weld Metal of the PVRUF Vessel*, USNRC Report NUREG/CR-6471, Vol. 2, U.S. Nuclear Regulatory Commission, Washington, D.C.
- [14] Schuster, G.J., Doctor, S.R., Crawford, S.L., and Pardini, A.F., 1999, *Characterization of Flaws in U.S. Reactor Pressure Vessels: Density and Distribution of Flaw Indications in the Shoreham Vessel*, USNRC Report NUREG/CR-6471, Vol. 3, U.S. Nuclear Regulatory Commission, Washington, D.C.
- [15] Simonen, F. A., Doctor, S. R., Schuster, G. J., and Dickson, T. L., “Distributions of Fabrication Flaws in Reactor Pressure Vessels for Structural Integrity Evaluations,” *Fatigue, Fracture, and Damage Analysis, Vol. II, ASME Pressure Vessels and Piping Conference*, Vancouver, British Columbia, Canada, August 2002, PVP-Vol. 443-2, pp. 133-143.
- [16] Williams, P. T., Bowman, K. O., Bass, B. R., and Dickson, T. L., “Weibull Statistical Models of K_{Ic}/K_{Ia} Fracture Toughness Databases for Pressure Vessel Steels with an Application to PTS Assessments of Nuclear Reactor Pressure Vessels,” *International Journal of Pressure Vessels and Piping*, **78**(2-3), (2001) pp. 165-178
- [17] Dickson, T. L., Williams, P. T., and Bass, B. R., “An Improved Probabilistic Fracture Mechanics Model for Pressurized Thermal Shock,” *Proceedings of Sixteenth International Conference on Structural Mechanics in Reactor Technology (SMiRT-16)*, Washington, DC, August 2001.